Cite this article
Domnich B, Shevhcuk D, Kirianchuk V and Voronov A
Biobased latex adhesives from isobornyl methacrylate and plant-oil-based acrylic monomers.
Green Materials,
https://doi.org/10.1680/jgrma.23.00070

Research Article
Paper 2300070
Received 12/07/2023; Accepted 17/08/2023
First published online 24/08/2023

Green Materials

Biobased latex adhesives from isobornyl methacrylate and plant-oil-based acrylic monomers

Bohdan Domnich MSc
Research Assistant, Department of Coatings and Polymeric Materials, North Dakota State University, Fargo, ND, USA

Oleg Shevhcuk PhD
Associate Professor, Department of Organic Chemistry, Institute of Chemistry and Chemical Technologies, Lviv Polytechnic National University, Lviv, Ukraine

Vasylyna Kirianchuk PhD
Research Scientist, Department of Coatings and Polymeric Materials, North Dakota State University, Fargo, ND, USA

Andriy Voronov PhD
Professor, Department of Coatings and Polymeric Materials, North Dakota State University, Fargo, ND, USA (corresponding author: andriy.voronov@ndsu.edu)

A range of cross-linkable latex copolymers with biobased content of up to 90% was synthesized from isobornyl methacrylate combined with acrylic monomers based on high-oleic soybean oil (HO-SBM) or camelina oil (CMM) through miniemulsion polymerization. By varying the HO-SBM and CMM macromolecular fractions, the cross-linking density of the resulting materials can be altered due to differences in the fatty acid profiles of the plant-oil-based monomers. The glass transition temperature of the synthesized copolymers correlates very well with the calculated Flory–Fox values. A higher cross-linking density of the biobased copolymer films leads to a notable growth in the modulus of the materials, while the elongation at break decreases due to more restricted macromolecular mobility. Remarkably, the copolymer with the highest unsaturation degree in the investigated range (based on CMM) shows an increase in both the modulus and elongation at break, due perhaps to extended entanglements of fatty-acid-based side chains. The adhesion performance of the cross-linked biobased copolymers was evaluated by performing shear and peel strength measurements on steel and polypropylene. Based on the obtained results, the unsaturation degree of CMM and HO-SBM (determined by plant oil composition) can be applied as a criterion for adjusting adhesion by choosing plant-oil-based monomers (or their mixtures) with different unsaturation degrees to achieve properties and performance required for specific applications.

Keywords: cross-linking density/green adhesives/high biobased content/miniemulsion terpolymerization/plant oils/renewable resources/UN SDG 12: Responsible consumption and production

Notation

d	density of the polymer (kg/m^3)
E	Young's modulus (in the tensile test) (MPa)
E'	storage modulus (in dynamic mechanical analysis) (MPa)
F_i	molar fraction of the corresponding monomer in the copolymer
I_x	integral value of a peak in a nuclear magnetic resonance spectrum
J	coupling constants
M_c	molecular weight between cross-links (g/mol)
M_i	molecular weight of the corresponding monomer
R	universal gas constant (J/(K mol))
T	temperature (K)
T_g	glass transition temperature (°C)
$T_{g\,calc}$	glass transition temperature calculated using the Flory–Fox equation (°C)
U_{MF}	unsaturation degree (allyl double bonds) of the monomer feed
U_p	unsaturation degree (allyl double bonds) of the copolymer
W_1	weight of the empty aluminum dish
W_2	weight of the aluminum dish before drying
W_3	weight of the aluminum dish after drying
W_4	weight of the dried sample
W_5	weight of the used latex sample
δ	chemical shifts of characteristic peaks
ε_b	elongation at break (in the tensile test) (%)
ν	cross-linking density (mol/cm^3)

1. Introduction

Biobased polymers continue to gain attention from and consideration by industry and academic researchers worldwide due to the safety and environmental friendliness of green materials compared with their conventional petroleum-based counterparts.[1] Among natural feedstocks, triglyceride plant oils (fatty acid triglycerides) are widely investigated as a promising sustainable resource for making renewable polymeric materials. Plant oils are abundant raw materials, while the chemical structure of triglycerides provides reactive functionalities, such as ester groups and unsaturated fatty acid double bonds. These groups can

be used to transform triglycerides into building blocks for subsequent polymerization through various chain growth mechanisms.[2] Plant oil triglycerides differ widely in terms of chemical composition, depending on the combination and contents of saturated and unsaturated fatty acids. Hence, the choice of plant oil determines the properties of the synthesized monomers and polymers thereof, which play a vital role in the potential application of the resulting polymeric materials.[3,4] Various synthetic methods for converting triglycerides into new monomers have been developed to enable industrial applications of plant-oil-based polymers.[5–10] Different polymerization mechanisms, such as free-radical, cationic and step growth, are applied to synthesize polyesters, polyamides and polyurethanes based on plant/vegetable oils.[5,7,11–14] For many years, plant oils have been used to prepare materials for various applications, such as those in the food and packaging industry and as lubricants, polymeric coatings and adhesives.[2,15]

Using plant-oil-based polymeric materials as adhesives can bring unique advantages.[16] Plant oil triglycerides contain long aliphatic fatty acid fragments, which enhance the material hydrophobicity and water resistance of adhesives when incorporated into formulations.[17,18] Moreover, the presence of fatty acid fragments in the adhesive provides the effect of plasticization, while the allyl double bonds of fatty acids can be used for post-polymerization curing, which improves the mechanical properties of the adhesive, specifically the cohesive strength.[19,20] The advantages of plant-oil-based adhesives can be leveraged in different areas, even though the market for biobased adhesives remains limited.[21,22] Reduced environmental impact can be expected using plant-oil-based adhesive formulations due to the biodegradation of fatty acid side chains in the polymer macromolecules.[23,24] In contrast, complete biodegradability of conventional polymers (in particular, acrylic polymers) remains challenging.[25]

Using biopolymers with adhesive capabilities, such as proteins and polysaccharides, is a common way to introduce sustainability to this type of material.[26] An alternative approach, which applies to plant-oil-based polymers, is to develop new monomers from oils and incorporate them into the synthesis of new biobased polymeric adhesives in combination with other counterparts. The latter solution may provide easier substitution of conventional counterparts to the new materials since other ingredients and equipment for the application can remain the same. Additionally, plant-oil-based polymeric materials can be applied together in existing adhesive formulations as sustainable, functional additives.

The authors' research group synthesized a library of new plant-oil-based acrylic monomers (POBMs) for free-radical polymerization and incorporated POBMs into biobased polymers and copolymers, including latexes synthesized through emulsion/miniemulsion.[27,28] POBMs undergo free-radical polymerization and, at the same time, retain reactive sites (the double bonds of unsaturated fatty acids) for post-polymerization cross-linking. The unsaturated double bond functionality of POBMs impacts the polymer molecular weight and favors the formation of cross-linked networks of varying densities after the curing process. The properties of POBM-based polymers can be tuned with the unsaturation degree of the fatty acid side chains, which varies depending on the chemical composition of plant oil used.[29–31] The viscoelastic behavior of the resulting polymer can be controlled with the amount of incorporated POBMs and final polymer T_g.[23,24] This way, proper balance between adhesion and cohesion can be achieved, which is beneficial for the mechanical properties and bonding strength of polymer adhesives from POBMs.

In a previous study by the authors, POBM fragments were incorporated into ternary latex copolymers to determine their adhesive capabilities on substrates differing in surface energy, such as poly(ethylene terephthalate) (PET), polypropylene (PP), bleached paperboard and paperboard top-coated with a clay mineral.[32] The best-performing latexes with up to 45 wt.% high-oleic soybean oil (HOSO)-based monomeric fragments demonstrated promising adhesive performance when bonding PET to PP and coated to uncoated paperboard substrate pairs. As a result, substrate failure instead of cohesive/adhesive break was observed.

The adhesive performance of POBM-based latexes can be adjusted by using plant-oil-based monomers with different degrees of unsaturation, which provides material properties required for specific applications. Motivated by the obtained results, the development of latex structural adhesives with a high biobased content was targeted in this study. For this purpose, a range of highly biobased latexes (biobased content of up to 90%) was synthesized from high-oleic soybean-oil-based monomer (HO-SBM) or camelina-oil-based monomer (CMM) (30–50%) with differing unsaturation degrees combined with *n*-butyl acrylate (BA) (10–30%) as a comonomer with a low T_g of the homopolymer and isobornyl methacrylate (IBOMA) (40%) as the rigid counterpart with a high T_g of the homopolymer (Figure 1(a)).

Camelina sativa (or camelina) is a winter or spring annual oilseed plant grown in different regions of Europe and Northern America. It is a short-season crop (up to 100 days to mature), is tolerant to cold weather and has a high oil content in seeds (up to 40%).[33,34] Camelina seeds are considered underexploited while currently gaining interest from academic and industrial researchers.[35] Since camelina oil (CLO) has limited usage for food purposes, it can become a sustainable and non-competing food industry source for various material demands, including biobased polymers.[36] Compared with other commodity seed oils, the high unsaturated fatty acid content (up to 90%) of CLO makes it a promising feedstock for various industrial applications because its molecules can be converted into monomers that can be polymerized using various chain growth mechanisms.[37] CLO has a high content of polyunsaturated α-linolenic acid and has monounsaturated 11-eicosenoic acid, which makes its chemical composition unique compared with those of soybean, sunflower, linseed and canola

oils, already widely considered in the manufacturing of biobased polymers and polymeric materials.

Produced by the esterification of camphene with methacrylic acid, IBOMA is an industrially established biobased monomer yielding homopolymers with a T_g above 150°C.[38–40] In this study, the copolymer composition was varied to investigate the potential of HO-SBM and CMM to replace petroleum-based BA in adhesive manufacturing. Additionally, the effect of the latex molecular weight distribution and degree of cross-linking predetermined by copolymer composition was studied.

The best-performing adhesives have balanced strength and ductility while showing a modulus similar to or lower than those of the substrates being bonded together.[41] In this work, the combination of low-T_g acrylates (BA and HO-SBM/CMM) provides the flexibility needed for peel strength, while high-T_g IBOMA fragments facilitate cohesive strength. Gradual replacement of BA with POBM may increase the cross-linking density (by varying the HO-SBM or CMM fraction in the copolymers) and enhance the cohesion strength required for structural adhesives.

HOSO and CLO have significantly different fatty acid profiles. The unsaturated fatty acids present in HOSO are α-linolenic acid ($C_{18:3}$), linoleic acid ($C_{18:2}$) and monounsaturated oleic acid ($C_{18:1}$). HOSO also contains saturated fatty acids, such as palmitic acid ($C_{16:0}$) and stearic acid ($C_{18:0}$). The fatty acid composition of CLO differs with a significantly higher level of polyunsaturated fatty acids (linoleic acid and α-linolenic acid) compared with that of HOSO. CLO also contains monounsaturated 11-eicosenoic acid ($C_{20:1}$), which is not present in HOSO (Figure 1(b)).

The authors hypothesized that the unsaturation degree of the used plant oils could be considered a criterion for determining the effects of the POBM chemical composition on the adhesion properties of copolymers by changing the polymer molecular weight and cross-linking density.

2. Materials and methods

2.1 Materials

The chemicals used were HOSO (ReNu Source, Hartville, OH, USA), CLO (H&B Oils Center Co., Westchester, IL, USA), *N*-(hydroxyethyl)acrylamide (stabilized with mequinol, >98%) (TCI America, Chemical Abstracts Service (CAS) 7646-67-5), magnesium sulfate (anhydrous, reagent grade) (VWR Chemicals, Solon, OH, USA, CAS 7487-88-9), sodium dodecyl sulfate (SDS, $C_{12}H_{25}SO_4Na$; biotechnology grade) (VWR Chemicals, Solon, OH, USA, CAS 151-21-3), BA (>99.0%) (TCI America, Portland, OR, USA, CAS 141-32-2), IBOMA (technical grade) (Sigma-Aldrich, St. Louis, MO, USA, CAS 7534-94-3), acrylic acid (AA; 99%) (Alfa Aesar, Heysham, UK, CAS 79-10-7) and azobisisobutyronitrile (AIBN; $[(CH_3)_2C(CN)]_2N_2$, 98%) (Sigma-Aldrich, St. Louis, MO, USA, CAS 78-67-1). The driers and curing catalysts used were cobalt Ten-Cem (12%) (OM Group (OMG), Westlake, OH, USA, OMG code 115105), zirconium Hex-Cem (12%) (OMG, Westlake, OH, USA, OMG code 115361), calcium Hydro-Cem (5%) (OMG, Westlake, OH, USA, OMG code 115083) and Dri-Rx HF (OMG, Westlake, OH, USA, OMG code 115409). All used solvents were reagent grade or better and used as received. Deionized water was used throughout the study (Milli-Q water, Millipore, 18 MΩ). Clear moisture-resistant PET film (McMaster-Carr), QD-36 smooth-finish steel panels (Q-Lab) and clear PP sheets (McMaster-Carr) substrates were used.

2.2 Synthesis of CMM

CMM was synthesized using a reaction pathway previously reported elsewhere by this research group for other plant-oil-based monomers.[29,30] In brief, about 115 g of *N*-(hydroxyethyl)acrylamide was added to 150 g of CLO (with an acrylamide alcohol-to-triglyceride molar ratio of 5.9:1), 150 ml of tetrahydrofuran (THF) and 0.1 g of 2,6-di-*tert*-butyl-*p*-cresol in a two-necked 500 ml round-bottom flask equipped with a mechanical stirrer. The reaction mixture was heated to 40°C in the presence of a catalytic amount of ground sodium hydroxide (1.5 g), which was added to the reaction mixture with continuous stirring. The reaction mixture was stirred at 40°C until complete homogenization (approximately 3 h) and afterward diluted with hexane and purified by washing with brine. The remaining water was removed using anhydrous magnesium sulfate, while the rest of the solvents were evaporated under a vacuum, yielding about 170 g of acrylic monomer (94–96% of the theoretical yield). The resulting monomer contained one acrylic double bond linked to one fatty acid chain, mainly unsaturated linoleate with two allyl carbon double bonds, and also monounsaturated oleate, triunsaturated linolenate and saturated fatty acid residues (Figure 1(a)). Synthesis and characterization of HO-SBM has been reported elsewhere.[29,32]

2.3 Synthesis of the HO-SBM/CMM-based latexes

Batch miniemulsion polymerization was used for the synthesis of latexes. The oil phase and aqueous phase were prepared first to

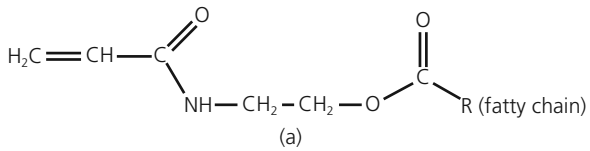

(a)

R (C:D)	16:0	18:0	18:1	20:1	18:2	18:3
HOSO	4–5	3–4	74–76	–	12–14	3–5
CLO	3–8	2–3	14–16	12–15	15–23	31–40

(b)

Figure 1. (a) Chemical structures of HO-SBM and CMM; (b) compositions of HOSO and CLO (in mol.%). R (C:D) is the structure of the fatty acids (C is the number of carbon atoms in the fatty acid chain, and D is the number of double bonds in the fatty acid)

perform the process. A typical recipe for latex is presented in Table 1.

First, the oil phase (28 g) was prepared by mixing the monomers HO-SBM or CMM (30–50 wt.%, 8.4–14 g), BA (30–10 wt.%, 8.4–2.8 g) and IBOMA (38 wt.%, 10.8 g), and AA (1 wt.%, 0.28 g) was added as an adhesion promoter with the oil-soluble initiator AIBN (1.5 wt.% per oil phase, 0.4 g). For the aqueous phase, SDS (5 wt.% per oil phase, 1.4 g) and sodium chloride (NaCl) (0.1 wt.% per aqueous phase, 0.05 g) were mixed with Millipore water (65 wt.% of the total latex prepared, 52 g). A miniemulsion was formed using ultrasonication (Qsonica Q500 sonicator, 500 W, 0.5 inch (12.7 mm) tip, 20 kHz) of the pre-emulsion with three 60 s cycles of sonication and 30 s rest cycles between them. An ice bath was used to cool down the mixture during the sonication process to avoid overheating and premature polymerization. The prepared miniemulsion was transferred to a dry flask, purged with ultra-high-purity nitrogen, subsequently polymerized for 12 h at 70°C and magnetically stirred at 330 revolutions/min.

The solid content of all latexes was maintained at 35 wt.%. After the synthesis, the latexes were cooled to room temperature, filtered into glass vials using cheesecloth to remove possible coagulum and stored under ambient conditions.

2.4 Characterization of POBM-based latexes

2.4.1 Conversion

After the synthesis, the solid content and conversion were determined gravimetrically. To measure the solid content, about 1 ml of latex was placed on an aluminum dish and dried to a constant weight in an oven at 120°C. For conversion measurement, about 1 ml of latex was precipitated in 6 ml of methanol to remove unreacted monomers. Multiple precipitations were performed to achieve complete monomer removal. The purified copolymer was dried in the oven at 120°C to constant weight. Any coagulated residue was collected on an aluminum dish and dried in the oven at 120°C until constant weight. The coagulum amount was calculated as a wt.% of the total weight of the oil phase. The solid content and conversion were calculated using Equations 1 and 2, respectively:

$$\text{Solid content } (\%) = \frac{W_3 - W_1}{W_2 - W_1} \quad (1)$$

where W_1 is the weight of the empty aluminum dish and W_2 and W_3 are the weights of the dish before and after drying, respectively.

$$\text{Conversion } (\%) = \frac{\text{Solid content} \times W_4}{W_5} \quad (2)$$

where W_4 is the weight of the dried sample and W_5 is the weight of the used latex sample.

Table 1. Typical recipe for miniemulsion copolymerization

	%	%	Mass: g
Oil phase	35		28
HO-SBM/CMM		30–50	8.4–14
BA		30–10	8.4–2.8
IBOMA; AA		39; 1	10.92; 0.28
Initiator, AIBN: % per oleo phase		1.5	0.42
Aqueous phase	65		52
Emulsifier, SDS: wt.% per oleo phase		5	1.4
Sodium chloride (NaCl): wt.% per aqueous phase		0.1	0.052
Total	100		80

2.4.2 Dynamic light scattering

The latex particle size and particle size distribution were measured using a Nicomp 380 submicron particle sizer with a 12 mW laser diode at fixed detection angle of 90°. To prepare the sample, one drop of latex was diluted in approximately 20 ml of deionized water. If necessary, the obtained sample was further diluted during the analysis.

2.4.3 Nuclear magnetic resonance analysis

The copolymer composition was analyzed using hydrogen-1 (^{1}H) nuclear magnetic resonance (NMR) spectroscopy (Avance III HD 400 high-performance digital NMR spectrometer, Bruker, Billerica, MA, USA) with deuterated chloroform ($CDCl_3$) as a solvent. Samples were prepared by dissolving 0.01 g of the dried polymer in 0.7 ml of deuterated chloroform. The same procedure was employed to determine the fatty acid composition of plant oils and synthesized POBMs.

2.4.4 Fourier transform infrared spectroscopy

To confirm the chemical structure of the synthesized POBMs and compare them with the chemical structures of the used plant oils, a Thermo Scientific Nicolet 8700 Fourier transform infrared (FTIR) spectrometer was used in transmittance mode. Samples of plant oils and POBMs in liquid state were applied as a thin film on a potassium bromide (KBr) crystal and scanned in the 3800–500 cm^{-1} wave number range. Then, the respective transmittance spectra of plant oils, POBMs and *N*-(hydroxyethyl)acrylamide were compared, and the presence of functional groups was confirmed.

2.4.5 Gel permeation chromatography

The average molecular weight and polydispersity of the synthesized biobased copolymers were determined using a Tosoh Bioscience EcoSEC HLC-8320 instrument, which consists of a Waters 1515 high-performance liquid chromatography pump, a Waters 2410 refractive index detector and two 10 µm PL-gel mixed-B columns (porous polystyrene/divinylbenzene cross-

linked matrix). The samples were eluted at a flow rate of 0.35 ml/min, and the column temperature was set at 40°C using THF as a carrier solvent. An EasiVial polystyrene standard was used to create a calibration curve. To prepare samples, 0.015 g of the polymer was dissolved in 3 ml of THF and filtered through a 0.22 µm poly(vinylidene fluoride) filter before injection.

2.4.6 Differential scanning calorimetry

The glass transition temperature of copolymers was measured using differential scanning calorimetry (DSC) (TA Instruments DSC 2500 calorimeter). A dried polymer sample (5–10 mg) was placed into a standard DSC aluminum crucible. Measurements were performed under dry nitrogen with a flow rate of 50 ml/min in heat/cool/heat mode at a heating/cooling rate of 10°C/min. To determine T_g, the midpoint of the inflection region observed in the second heating cycle was considered.

2.4.7 Gel content

The gel content of polymers was measured using a solvent-extraction method. Dried polymer samples (around 0.2 g) were placed into cellulose extraction thimbles (18 × 55 mm), weighed and put into a Soxhlet extractor. The extraction process was performed for 24 h using toluene as a solvent. After the extraction, the cellulose thimbles were dried in the oven at 120°C to constant weight. The polymer gel content was calculated using the following equation:

$$\text{Gel content} = \frac{\text{weight of the dry gel}}{\text{weight of the dry polymer sample}} \quad (3)$$

2.5 Preparation of polymer films

To measure the mechanical properties of copolymers, cured polymer films were prepared. First, latex samples were precipitated in methanol to remove unreacted monomers. Multiple precipitations were performed to ensure complete monomer removal. Then, polymer was dried under a nitrogen atmosphere to remove methanol. The pure dried polymer was then dissolved in toluene to obtain a 30 wt.% solid content. To facilitate the cross-linking process through autoxidation, primary and secondary driers and catalysts were added at the necessary level to the polymer solution. Then, the polymer solution was drawn down on the polytetrafluoroethylene substrate to ensure easy release after curing. A dry film thickness of 100 µm was targeted, and the wet film thickness was adjusted accordingly based on the solid content of the formulation. Toluene was allowed to evaporate to obtain a solid tack-free film, and subsequent curing for 5 h at 100°C was performed. After curing, the samples were cooled down and stored under ambient conditions before testing.

2.6 Mechanical characterization (tensile test)

Cured polymer films were cut into rectangle-shaped samples with dimensions of 25 × 5 mm. The thickness of the films was measured using a digital micrometer before each test. An Instron 5542 tensile tester was used at a constant test speed of 5 mm/min. The sample was fixed in the clamps to obtain a 10 × 5 mm test area and was pulled at constant speed until film failure. Young's modulus was calculated as a slope of the stress–strain curves on a tensile diagram when the material undergoes elongation in elastic mode (0.1–1.0% elongation). The reported Young's modulus and elongation at break values were the averages of at least five measurements.

2.7 Dynamic mechanical analysis

To measure the cross-linking density (ν) and average molecular weight of the polymer chains between two cross-linking points in a cross-linked network (M_c) of the cured films, a DMA 850 (TA Instruments) dynamic mechanical analyzer in tension mode was used. The sample preparation procedure was the same as for the tensile test, except for the sample dimensions, which were 25 × 5 mm. The dynamic mechanical analysis (DMA) measurements were performed by heating the sample from −40 to 150°C at a rate of 5°C/min under a constant frequency of 1 Hz. Based on the rubber elasticity theory, at small deformations, the polymer cross-linking density is proportional to the storage modulus. Therefore, ν can be calculated using the value of the tensile storage modulus E' in the rubbery plateau region using the following equation:

$$\nu = \frac{E'}{3RT} \quad (4)$$

where R is the universal gas constant and T is the absolute temperature in kelvin at which E' is recorded. The value of T was taken at 60°C above T_g, calculated as the peak of tan δ.

Then, based on the same theory, M_c can be calculated using the following equation:

$$M_c = \frac{3dRT}{E'} = \frac{d}{\nu} \quad (5)$$

where R is the universal gas constant; T is the absolute temperature in kelvin at which E' is recorded; and d is the polymer density.

To calculate the polymer density, rectangle-shaped samples were prepared. The dimensions of the samples were measured using a caliper, and the volume was calculated. The mass was measured with a digital balance, and the density was calculated using the volume and mass of the sample.

2.8 Adhesion performance testing of copolymers

The peel and shear strengths of the synthesized copolymers as structural adhesives were measured according to the American Society for Testing and Materials (ASTM) D 3330[42] and D 1002-10[43] standards, respectively. An MTS Insight Electromechanical 5 kN extended length-testing system with load cell of 5 kN was used in all tests.

2.9 Preparation of structural adhesives

Identical formulations used to obtain polymer films were prepared for adhesion testing. Before the film application, the PET substrate was cleaned with deionized water and dried. Then, corona treatment was performed using a Tantec sheet corona treater with 1 kV energy applied to increase the polarity of the polymer substrates and promote adhesion. To avoid degradation of the substrate because of the high energy applied, the exposure time was decreased and multiple cycles of treatment were performed instead. Immediately after the treatment, a 500 µm thick film was applied from the toluene solution to the PET substrate using a casting knife film applicator, targeting a dry film thickness of 150 µm. The adhesive film was dried under ambient conditions until complete evaporation of toluene, and a second substrate was applied to create an adhesive joint. The bonding area was compressed with a hand roller to ensure bonding along two substrates and exclude inhomogeneities. The 180° peel test bonding area between the two substrates was 50 × 127 mm, which was cut into 10 mm wide samples after curing. For the lap shear test, samples with a bond area of 25 mm^2 were prepared.

Compared with polymer film curing, adhesive curing through autoxidation was challenging because of the limited oxygen diffusion through the substrates. Cross-linking conditions were set as 8 h at 120°C to ensure complete curing of the bonds, while the decomposition temperature of used materials was much higher, and there was no risk of their degradation.

2.10 The 180° peel test

The peel strength of adhesives was tested on the PP and steel substrates, which were significantly different in terms of the surface free energy and PP being less polar than steel. Samples were tested the same day after curing. Before testing, samples were cut into 10 mm wide strips, yielding five samples for each test. The solid substrate (PP or steel panel) and PET backing were fixed in the test grips of the tension testing machine. A load at a constant head speed of 5 mm/s was applied. The autographic recording of load against distance peeled was made during the peel test. The peel resistance was measured over a length of at least 100 mm of the bond line after the initial peak was determined, and the value in 20–80% of the working range was used for calculations. The measurement of peel strength was repeated five times, and the average value was reported.

2.11 Lap shear test

Two ends of the sample were fixed in the grips, and a load at a constant speed of 1 mm/s was applied. The diagram of the applied load against extension was recorded, and the maximum applied force during the test was reported as shear strength. The measurement was repeated five times, and the average value was reported.

3. Results and discussion

3.1 Synthesis and characterization of CMM

Using the method of plant oil direct transesterification developed by the authors' group, CMM was synthesized and then incorporated into chain copolymerization with BA and IBOMA to compare their properties and adhesive performance with latexes made of significantly less unsaturated HO-SBM (Figure 2).

The CMM chemical structure was confirmed by FTIR and hydrogen-1 NMR spectroscopy. According to the FTIR spectroscopy data, the appearance of strong absorption bands at 3400–3200 cm^{-1} (NH bonds), 1670 cm^{-1} (carbonyl group, amide I)

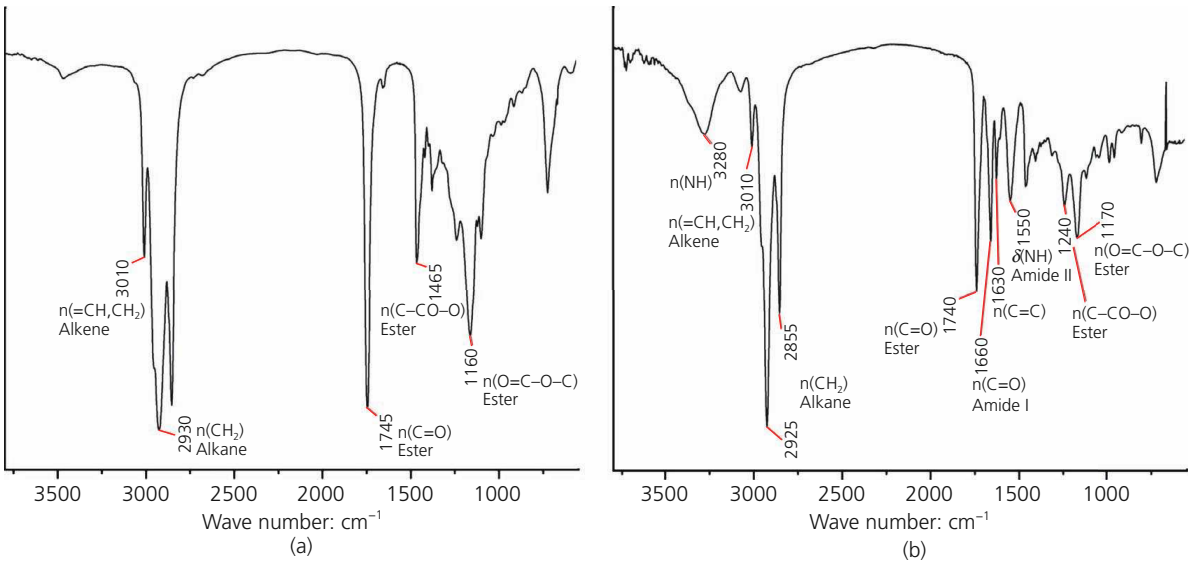

Figure 2. FTIR spectra of (a) CLO and (b) CMM

and 1540 cm^{-1} (NH, amide II) in the spectrum of the CMM (Figure 2(b)), when compared with the spectrum of the oil (Figure 2(a)), indicates the addition of fatty acid acyl moieties to the acrylamide fragment. The absorption bands at 1740, 1245 and 1180 cm^{-1} confirm the presence of an ester group in the CMM molecule. The absorption bands at 1665–1635 cm^{-1} indicate the presence of a carbon–carbon double bond in the fatty acid chains.[28]

The hydrogen-1 NMR spectra of the CMM and CLO are shown in Figure 3(a) and 3(b), respectively, with annotation of chemical shifts (δ) of characteristic peaks and their coupling constants (J). The characteristic peaks at 6.27–6.31, 6.06–6.13 and 5.65–5.68 parts per million (ppm) (A, B, D, 3H) correspond to the presence of protons in the acrylic double bond of the acryloylamide moiety. The peaks at 4.20–4.22 and 3.59–3.63 ppm indicate the presence of the protons of two methylene groups between the amide and ester groups of the CMM. The peaks in the range from 0.86 to 2.81 ppm correspond to the protons in the fatty acid fragments, whereas the peaks at 5.29–5.41 ppm indicate the presence of protons at the carbon–carbon double bonds. The peaks at 1.98–2.11 ppm correspond to protons in the α-position to the double bond (allylic hydrogen), which can undergo chain-transfer reaction, triggering the polymerization retardation.[28]

The content of fatty acid chains in the CMM mixture produced by the transesterification of CLO with *N*-(hydroxyethyl)acrylamide was determined by calculating the ratio of the integral values in the hydrogen-1 NMR spectra of the CLO and the resulting monomer mixture (Figure 4).

According to the calculations based on hydrogen-1 NMR spectroscopy data, the monomer mixture consists of saturated fatty acid fragments ($C_{18:0}$ and $C_{16:0}$), 17.9% (stearic and palmitic); oleic acid fragments ($C_{18:1}$), 23.9%; linoleic acid fragments ($C_{18:2}$), 41.6%; and linolenic acid fragments ($C_{18:3}$), 18.7%, after the CLO transesterification. Therefore, the predominant component of the CMM is a molecule with linoleic acid fragments – 2-*N*-acryloyl aminoethyl linoleate. To quantify the unsaturation degree of the CMM, determined by the number of double bonds in the fatty acid chains, the iodine value of the monomer and CLO used for the synthesis was determined. The iodine value of the CMM (155 g/100 g) is higher than that of the oil (144 g/100 g) due to the unsaturated acryloyl amide moiety incorporated during transesterification.

3.2 Synthesis and characterization of highly biobased latex copolymers

In this work, latexes with up to a 90 wt.% biobased content were synthesized from monomer mixtures containing HO-SBM or CMM (30–50 wt.%) combined with IBOMA (40 wt.%) and BA (10–30 wt.%) using miniemulsion polymerization (Table 2). The latter process is widely used for the (co)polymerization of poorly water-soluble monomers.[30] Considering the high hydrophobicity of HO-SBM, CMM and IBOMA, the miniemulsion process was employed in this study.

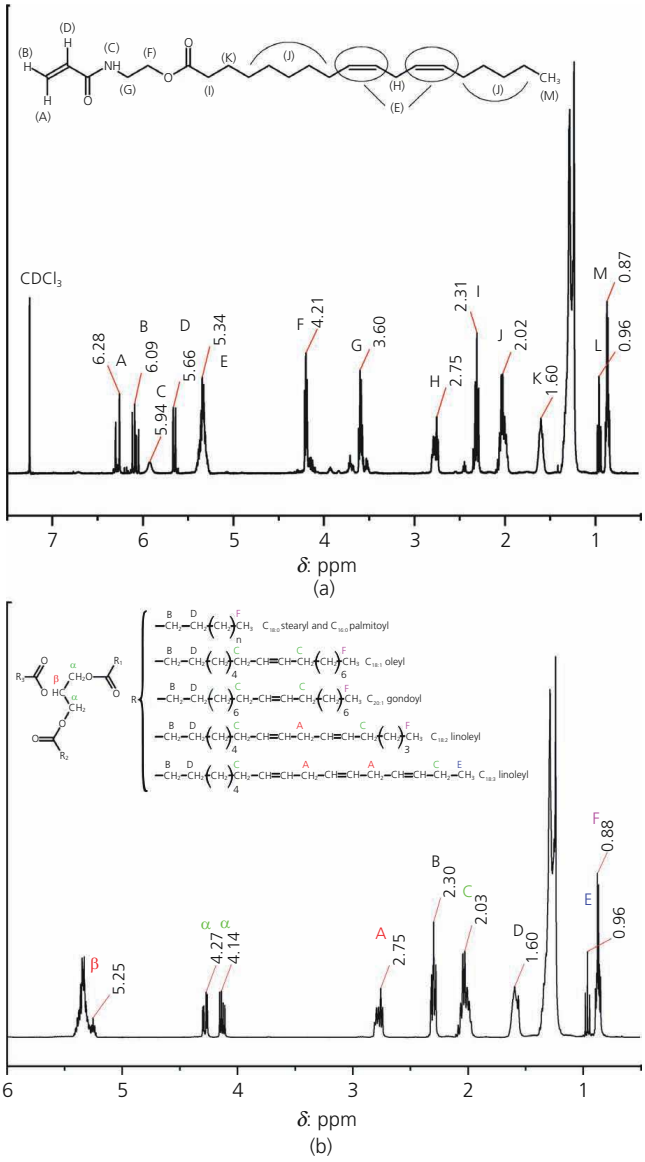

Figure 3. (a) Hydrogen-1 NMR spectrum of CMM ($CDCl_3$, 400 MHz): δ 6.27–6.31 (dd, 1H, J_{AD} = 17 Hz, J_{AB} = 1.6 Hz), 6.06–6.13 (dd, 1H, J_{DA} = 17 Hz, J_{DB} = 10.4 Hz), 5.94 (m, 1H), 5.65–5.68 (dd, 1H, J_{BD} = 10.2 Hz, J_{BA} = 1.2 Hz), 5.29–5.41 (m, 2H), 4.20–4.22 (t, 2H, J = 5.6 Hz), 3.59–3.63 (q, 2H, J = 5.6 Hz), 2.75–2.81 (m, 2H), 2.30–2.34 (t, 2H, J = 7.6 Hz), 1.98–2.11 (m), 1.58–1.63 (m), 0.95–0.99 (t, 3H, J = 7.6 Hz), 0.86–0.90 (m, 3H). (b) Hydrogen-1 NMR spectrum of CLO: 5.22–5.27 (m, 1H), 4.26–4.30 and 4.11–4.15 (dd, 2H, J = 6 Hz), 2.74–2.81 (m), 2.28–2.32 (t, 2H, J = 7.6 Hz), 1.97–2.08 (m), 1.56–1.61 (m, 2H), 0.94–0.98 (t, 3H, J = 7.6 Hz), 0.85–0.89 (m, 3H)

Table 2 shows the monomer feed, latex characteristics and chemical composition of latex copolymers calculated using hydrogen-1 NMR spectroscopy (Figure 5(a)). In the POBM–BA–IBOMA copolymer spectrum, the peaks at 4.27–4.73 ppm correspond to the proton of IBOMA (b, 1H). The peaks at 3.07–3.85 ppm are assigned to the protons in the

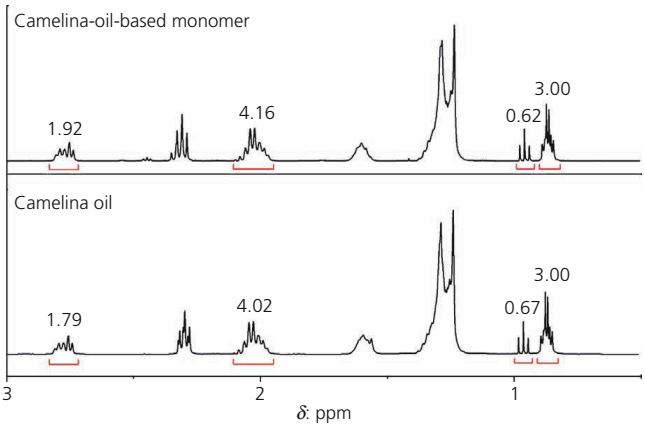

Figure 4. Hydrogen-1 NMR spectra of CLO and CMM

methylene group located next to the amide in POBM (a, 2H). BA repeating units are represented by the protons of the methylene group next to the ester group at 3.85–4.26 ppm (c, 2H). However, the characteristic peaks of BA protons overlap with those of the protons in the methylene group located next to the ester group in POBMs (d, 2H) at the same spectral range 3.85–4.26 ppm, which complicates the calculation process.

To obtain the integral of the BA characteristic peak (I_c), the integral value of the POBM homopolymer peak (I_d) at 3.85–4.26 ppm was subtracted from the integral of the cumulative peak of BA and POBM (I_{c+d}) in the copolymer at the spectral range 3.85–4.26 ppm. Calculations of copolymer compositions were performed based on the integrals of characteristic peaks (I_a, I_b, I_c) using the following equations:

$$6.\quad [\text{POBM}] : [\text{BA}] : [\text{IBOMA}] = \frac{I_b/2}{I_t} : \frac{I_c/6}{I_t} : \frac{I_a/5}{I_t}$$

$$7.\quad I_t = \frac{I_b}{2} + \frac{I_c}{6} + \frac{I_b}{5}$$

The mass compositions of the copolymers were calculated using the following equation and compared with the monomer feed in Table 2:

$$8.\quad [\text{POBM}] : [\text{BA}] : [\text{IBOMA}] = \frac{F_1 M_1}{F_t} : \frac{F_2 M_2}{F_t} : \frac{F_3 M_3}{F_t}$$

where F_i is the molar fraction of the corresponding monomer in the copolymer; M_i is the molecular weight of the corresponding monomer; and F_t is $\sum_{i=1} F_i M_i$.

As it was determined, the biobased content in the latex copolymers ranges from 70 to 90 wt.%. For each copolymer, the unsaturation degrees of a monomer feed (U_{MF}) and the resulting copolymer (U_p) were calculated from the numbers of the C=C double bonds in the fatty acid fragments of the CMM and HO-SBM experimentally measured by hydrogen-1 NMR as described by Demchuk *et al.*[29] As Table 2 also shows, the majority (70–85%) of double bonds in fatty acid fragments are retained during the polymerization (indicated by the unsaturation value of the polymer, U_p). This indicates that fatty acid double bonds are readily available for post-polymerization reactions, particularly cross-linking of latex films.

The synthesized latexes with an average particle size of 50–150 nm exhibit high stability at room temperature for several months. Figure 5(b) shows that in experiments with higher concentrations of BA in the monomer feed, the latex particle size decreases, as does the particle size distribution. The latter observation can be the result of a mixed-nucleation mechanism. Assuming aqueous solubility of BA (0.15%), homogeneous nucleation (addition to droplet nucleation as a primary desired mechanism) seems to be a possible mode for latex particle formation in this study. In the experiments with a higher BA concentration (20 and 30 wt.%) in the feed, latex particle diameters decrease since more particles nucleate and become smaller in size.

Figure 6(a) shows that the molecular weight of the latex copolymers continuously decreases in a range corresponding to

Table 2. Properties of POBM-based latex polymer

Latex	Solid content: %	Monomer feed: wt.% (P-B-I)	Monomer conversion: %	Copolymer composition: wt.% (P-B-I)	U_{MF}/U_p	$T_g/T_{g\,calc}$: °C
HSB1	35.1	30–30–40	89.0	24–28–48	0.31/0.24	9/3
HSB2	34.8	40–20–40	87.6	34–20–46	0.41/0.35	20/–7
HSB3	34.6	50–10–40	84.8	42–10–48	0.51/0.43	25/–8
CML1	33.6	30–30–40	90.5	24–30–46	0.51/0.41	18/–1
CML2	32.9	40–20–40	79.5	27–20–53	0.68/0.46	34/10
CML3	34.6	50–10–40	64.1	35–12–53	0.86/0.60	36/5

P-B-I, POBM–BA–IBOMA

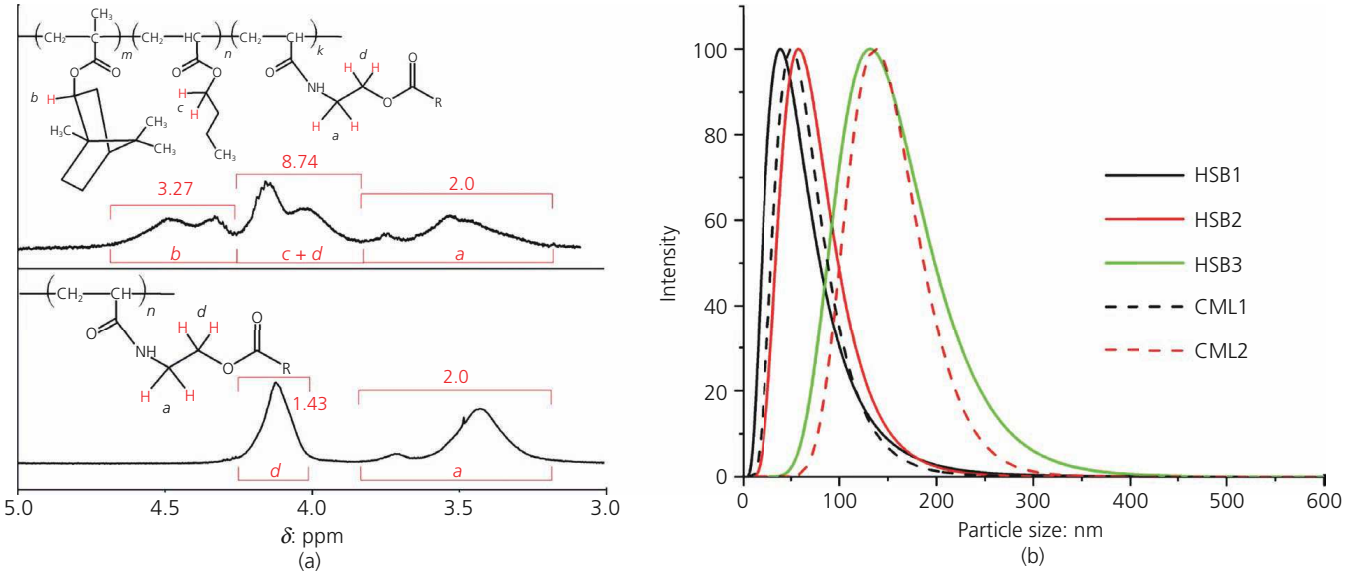

Figure 5. (a) Hydrogen-1 NMR spectra of the POBM–BA–IBOMA copolymer (top) and POBM homopolymer (bottom); (b) dynamic light scattering analysis of the biobased latexes

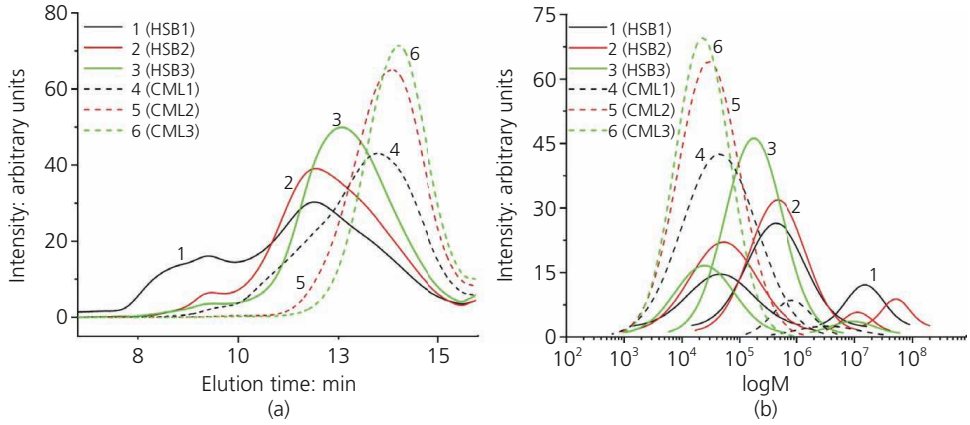

Figure 6. (a) Original plots of molecular weight distributions obtained from GPC analysis and (b) plots deconvoluted into molecular weight fractions

increasing unsaturation of the monomer feed. The decrease in molecular weight can be explained by the effect of degradative chain transfer on the HO-SBM/CMM monomer molecules, which differs depending on the number of allylic hydrogen atoms in the POBM molecules.[29] The authors previously observed this effect during copolymerization with an increase in the fraction of plant-oil-based monomers in the monomer feed, and the results are reported elsewhere.[28–30] The values of the chain-transfer constants of the monomers, determined earlier, clearly depend on the monomer structure (number of C–H groups in the α-position to the fatty acid double bonds) and increase with an increasing monomer unsaturation.[28] The extent of the chain-transfer reactions is more pronounced in the more unsaturated CMM.

At the same time, during the polymerization of BA, evidence of the formation of tertiary radicals by intramolecular chain transfer (back-biting, when growing macroradicals abstract the labile hydrogen located at two units back in the backbone) or intermolecular chain transfer (growing macroradical abstracts the labile hydrogen atom in acrylate in a dead polymer chain) to the polymer has been provided.[44–46] As a result, the molecular weight distribution of the final polymer may change significantly by forming short-chain branched polymers. Considering two chain-breaking reactions, the formation of linear macromolecules with fatty acid side groups, as well as branched macromolecules during latex synthesis, may be assumed. The authors distinguished different macromolecular populations in the latex copolymers after the deconvolution of the

original gel permeation chromatography (GPC) plots (Figure 6(b)). The identified fractions can correspond to linear (10^4–10^5 g/mol) and short-chain branched (10^6–10^7 g/mol) macromolecules. It is evident that branching becomes more pronounced when the concentration of BA in the initial monomer mixture increases. It is important to emphasize that the formation of cross-linked networks does not occur during synthesis because all synthesized copolymers remain soluble in the organic solvents. The ability to vary the contribution of each chain-breaking reaction during latex synthesis can be of particular interest as an experimental tool for varying the properties and performance of biobased latexes to be applied as adhesives.

3.3 Thermo-mechanical properties of latex copolymers

Generally, the glass transition temperature T_g dramatically affects the mechanical properties and performance of the polymer. As the authors previously reported, a controlled number of the non-polar long fatty acid side chains of a POBM decreases the amount of intermolecular interactions and allows tuning the copolymer T_g.[28–30] The presence of soft POBM and BA fragments in latex copolymers synthesized in this study decreases the T_g compared with that of the rigid poly(IBOMA) due to the internal plasticization effect in the copolymers.

While there is a difference between the chemical compositions of latex copolymers (as indicated in Table 2) obtained by DSC measurements, the values of T_g are comparable with theoretical values calculated using the Flory–Fox equation (Figure S1 in the online supplementary material). This indicates that the provided variations of the copolymer chemical composition do not significantly change the thermal properties of the final material. By minimizing the effect of T_g on the thermo-mechanical properties of the synthesized materials, the impact of U_{MF} and U_p on the thermo-mechanical properties of copolymers and their adhesion performance can be investigated in more detail. Based on DSC measurements, samples CML2 and CML3 were not considered further in this study for adhesive testing.

Thermoplastic and thermoset materials are differentiated based on macromolecular configuration. In thermoplastics, macromolecules are physically entangled and thus can be processed, reshaped and recycled with heating. Cross-linking can be applied to form macromolecular thermoset networks to increase the mechanical strength of the materials. When cross-linking is used (in particular to synthesize polymer structural adhesives), mechanical properties, such as elongation at break ε_b and Young's modulus E, are usually considered. Those properties are fundamentally determined using the cross-linking density, ν. Being a function of ν, the macromolecular mobility in a cross-linked network controls the material mechanical and thermal properties.

To eliminate the effect of unreacted monomers and surfactants on the thermo-mechanical and adhesion properties, all copolymers in this study were precipitated, and the pure polymer was used for further material characterization. Primary and secondary driers and catalysts were added to facilitate cross-linking. All polymer films were cured to a high cross-linking degree (75–80%), which was confirmed using Soxhlet extraction in toluene.

Table 3 shows the effect of U_{MF} on the experimentally determined cross-linking density, ν, and the effective molecular weight between cross-linking nodes (M_c) of cured latex films. Increasing the U_{MF} leads to an increase in ν and a decreased M_c. The presence of the more unsaturated CMM in the reactive mixture increases both U_{MF} and U_p compared with those of copolymers with HO-SBM. DMA plots of the cross-linked biobased latex films are shown in Figure S2 in the online supplementary material.

This leads to a sufficient increase in ν and a lower M_c because more sites for cross-linking reactions become available. A strong correlation is observed between U_{MF} and U_p and the mechanical properties of cross-linked polymer films based on HO-SBM. The value of M_c significantly decreases not only because of increasing ν but also due to the decreasing branched polymer fraction, leading to more compact packing of macromolecules. It is apparent that a higher ν brings remarkable growth in E, as the stress dissipates over more populated cross-linking nodes. However, the elongation at break decreases due to restricted macromolecular mobility. At the same time, the polymer film based on CMM (highest in a range of U_{MF} and U_p) shows a considerable increase in E while preserving a high elongation at break. This can be attributed to the formation of the polymer network with different (more entangled) morphologies, as many fatty acid fragments in CMM may have more than one cross-linking site.

Hence, the thermo-mechanical properties of polymer films based on HO-SBM/CMM and IBOMA depend considerably on the cross-linking density of the polymer network, which can be

Table 3. Properties of cured POBM-based copolymer films

	Biobased content (POBM/IBOMA): wt.%	Gel content: %	T_g by DMA: °C	ν: × 10^5 mol/cm^3	M_c: g/mol	E: MPa	ε_b: %
HO-SBM	24/48	74.5	40	2.6	39 500	15.9 ± 1.0	422 ± 29
	34/46	77.6	62	6.3	16 100	101.2 ± 15.1	177 ± 24
	42/48	79.7	69	8.2	12 400	141.8 ± 9.0	92 ± 19
CMM	24/46	80.3	73	7.2	13 200	182.3 ± 20.1	147 ± 25

controlled by the nature of incorporated plant-oil-based fragments, in particular their characteristic U_{MF} and U_p values.

3.4 Adhesion performance of highly biobased latex copolymers

To evaluate the feasibility of synthesized copolymers as structural adhesives, lap shear and 180° peel tests were performed. Two types of substrates were used – more polar steel and non-polar PP. Shear strength is the most crucial parameter for structural adhesives. To conduct a lap shear test, substrate joints between PET–steel and PET–PP were prepared according to the procedure described in Section 2. Corona treatment of both PET and PP substrates was used to increase the surface energy of substrates and promote adhesion. Shear strength is directly related to the material cohesive strength, meaning, in general, the higher cross-linking enhances the shear performance. Based on the obtained results (Figure 7), one can see an increase in shear strength on steel substrate with an increasing U_p.

It was also essential to consider the mode of bonding failure. Adhesive failure was observed for HSB1, while substrate failure occurred for some of the HSB2 replicates. For HSB3 and CML1, entirely substrate failure was observed for all replicates. There was no such evident correlation between shear strength and U_p for PET–PP substrate bonding. It was more challenging to bond two dissimilar polymeric materials with low roughness and low surface energy. Although corona treatment was employed to promote adhesion, other methods of substrate pretreatment, such as etching or mechanical scratching, might increase the bond strength.

Peel strength requires increased flexibility of the bonding material and is referred to as adhesion strength, which is typically opposite to the shear strength. Finding a proper balance between bond flexibility and strength is a challenging problem to solve, and most of the time, one of the properties should be diminished to maintain the high performance of a necessary one. As can be seen from the plot of peel strength (Figure 8) on steel and PP, this property of HO-SBM/CMM adhesives is inversely proportional to the unsaturation degree U_p. It is obvious that an increase in cross-linking density decreases the flexibility of the bond and, thus, peel strength. Interestingly, for HSB1 copolymer adhesive, failure of bonding occurred, while for all other samples, stick-slip failure was predominant. The latter is characteristic for the experiments in a specific range of test speeds or temperatures. Nevertheless, a change in failure mode was not observed in a significant range of test speeds (0.5–20 mm/s).

The obtained results show that the unsaturation degree of the used plant oils can be considered a criterion for determining the effects of the POBM chemical composition on the adhesion properties of copolymers by changing the cross-linking density. The adhesive performance of POBM-based latex copolymers can be adjusted by using plant-oil-based monomers with different degrees of unsaturation, which provides adhesive properties required for specific applications.

4. Conclusion

Miniemulsion polymerization of IBOMA and BA combined with HO-SBM or CMM was applied to synthesize latex copolymers with a biobased content of up to 90 wt.% to demonstrate their feasibility as cross-linked structural adhesives. By varying the HO-SBM and CMM macromolecular fractions, the cross-linking density of the materials could be changed due to differences in the fatty acid profile of plant-oil-based monomers. The molecular weight of the latexes decreased with increasing unsaturation in the monomer feed due to degradative chain transfer on the HO-SBM/CMM molecules. With that, the extent of the chain transfer was more pronounced for the more unsaturated CMM.

The mechanical properties of the cross-linked polymer films correspond to the unsaturation in the feed (determined by the CMM/HO-SBM fraction). A higher cross-linking density leads to

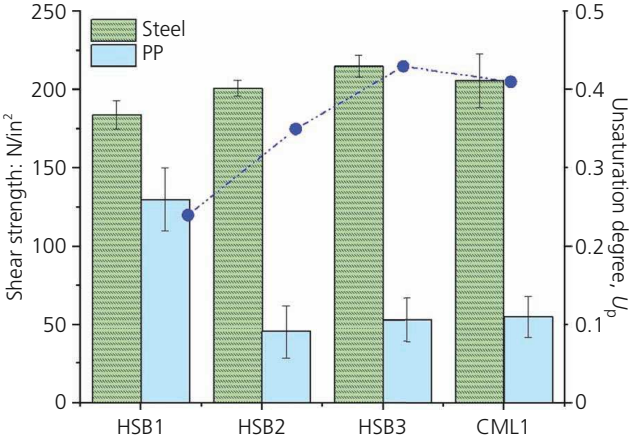

Figure 7. Shear strengths of HO-SBM/CMM adhesives on steel and PP substrates. 1 N/inch^2 = 1.55 kN/m^2

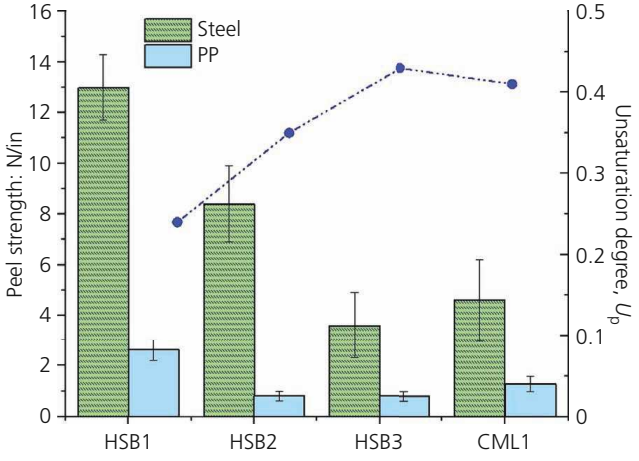

Figure 8. Peel strength of HO-SBM/CMM adhesives on steel and PP substrates. 1 N/inch = 39.4 N/m

notable growth in modulus, while the elongation at break decreases due to more restricted macromolecular mobility. The latex copolymer based on CMM with the highest unsaturation range shows considerable increases in both the modulus and elongation at break, possibly due to more extended entanglements of fatty acid side chains.

The utility of copolymers as adhesives and the effect of unsaturation on adhesion performance were studied using shear and peel strength measurements on steel and PP substrates. With increasing unsaturation, a shear strength increase was observed on steel, while no evident correlation was obtained for experiments on a smooth hydrophobic PP substrate. As expected, the peel strength on steel and PP was inversely proportional to the unsaturation degree in copolymers. Increasing the cross-linking density affected the flexibility of the bond materials, causing peel strength loss.

The obtained results show that the unsaturation degree of CMM and HO-SBM (determined by plant oil composition) can be considered a criterion for adjusting adhesion by using plant-oil-based monomers (or their mixtures) with different degrees of unsaturation to provide adhesive performance and properties required for specific applications.

Acknowledgements

This work was financially supported by the North Dakota (ND) Soybean Council, ND Department of Agriculture, Agricultural Products Utilization Commission and Center for Bioplastic and Biocomposites, which the authors acknowledge.

REFERENCES

1. Jospeh TM, Unni AB, Joshy KS *et al.* (2023) Emerging bio-based polymers from lab to market: current strategies, market dynamics and research trends. *Journal of Carbon Research* **9(1)**: article 30, https://doi.org/10.3390/c9010030.
2. Lligadas G, Ronda JC, Galià M and Cádiz V (2013) Renewable polymeric materials from vegetable oils: a perspective. *Materials Today* **16(9)**: 337–343, https://doi.org/10.1016/j.mattod.2013.08.016.
3. Guner FS, Yagci Y and Erciyes AT (2006) Polymers from triglyceride oils. *Progress in Polymer Science* **31**: 633–670, https://doi.org/10.1016/j.progpolymsci.2006.07.001.
4. Liu F and Zhu J (2015) Plant oil-based polymeric materials and their application. In *Green Materials from Plant Oils* (Liu Z and Kraus G (eds)). Royal Society of Chemistry, London, UK, vol. 29, pp. 93–126.
5. Xia Y and Larock RC (2010) Vegetable oil-based polymeric materials: synthesis, properties, and applications. *Green Chemistry* **12(11)**: 1893–1909.
6. Zhang C, Garrison TF, Madbouly SA and Kessler MR (2017) Recent advances in vegetable oil-based polymers and their composites. *Progress in Polymer Science* **71**: 91–143, https://doi.org/10.1016/j.progpolymsci.2016.12.009.
7. Mosiewicki MA and Aranguren MI (2016) Recent developments in plant oil based functional materials. *Polymer International* **65(1)**: 28–38, https://doi.org/10.1002/pi.5033.
8. Kunduru KR, Basu A, Zada MH and Domb AJ (2015) Castor oil-based biodegradable polyesters. *Biomacromolecules* **16(9)**: 2572–2587, https://doi.org/10.1021/acs.biomac.5b00923.
9. Miao S, Wang P, Su Z and Zhang S (2014) Vegetable-oil-based polymers as future polymeric biomaterials. *Acta Biomaterialia* **10(4)**: 1692–1704, https://doi.org/10.1016/j.actbio.2013.08.040.
10. Llevot A (2017) Sustainable synthetic approaches for the preparation of plant oil-based thermosets. *Journal of the American Oil Chemists' Society* **94(2)**: 169–186, https://doi.org/10.1007/s11746-016-2932-4.
11. Biermann U, Bornscheuer U, Meier M, Metzger JO and Schäfer HJ (2011) Oils and fats as renewable raw materials in chemistry. *Angewandte Chemie International Edition* **50(17)**: 3854–3871, https://doi.org/10.1002/anie.201002767.
12. Meier MAR (2018) Plant-oil-based polyamides and polyurethanes: toward sustainable nitrogen-containing thermoplastic materials. *Macromolecular Rapid Communications* **40(1)**: article 1800524, https://doi.org/10.1002/marc.201800524.
13. de Espinosa LM and Meier MAR (2011) Plant oils: the perfect renewable resource for polymer science?! *European Polymer Journal* **47(5)**: 837–852, https://doi.org/10.1016/j.eurpolymj.2010.11.020.
14. Pfister DP, Xia Y and Larock RC (2011) Recent advances in vegetable oil-based polyurethanes. *ChemSusChem* **4(6)**: 703–717, https://doi.org/10.1002/cssc.201000378.
15. Vieira MGA, da Silva MA, dos Santos LO and Beppu MM (2011) Natural-based plasticizers and biopolymer films: a review. *European Polymer Journal* **47(3)**: 254–263, https://doi.org/10.1016/j.eurpolymj.2010.12.011.
16. Finlay MR (2003) Old efforts at new uses: a brief history of chemurgy and the American search for biobased materials. *Journal of Industrial Ecology* **7(3–4)**: 33–46, https://doi.org/10.1162/1088198033230 59389.
17. Kong X, Liu G and Curtis JM (2011) Characterization of canola oil based polyurethane wood adhesives. *International Journal of Adhesion and Adhesives* **31(6)**: 559–564, https://doi.org/10.1016/j.ijadhadh.2011.05.004.
18. Saetung A, Rungvichaniwat A, Tsupphayakornake P *et al.* (2016) Properties of waterborne polyurethane films: effects of blend formulation with hydroxyl telechelic natural rubber and modified rubber seed oils. *Journal of Polymer Research* **23(12)**: article 264, https://doi.org/10.1007/s10965-016-1160-9.
19. Li C, Xiao H, Wang X and Zhao T (2018) Development of green waterborne UV-curable vegetable oil-based urethane acrylate pigment prints adhesive: preparation and application. *Journal of Cleaner Production* **180**: 272–279, https://doi.org/10.1016/j.jclepro.2018.01.193.
20. Li Y, Chou SH, Qian W *et al.* (2017) Optimization of soybean oil based pressure-sensitive adhesives using a full factorial design. *Journal of the American Oil Chemists' Society* **94(5)**: 713–721, https://doi.org/10.1007/s11746-017-2966-2.
21. Petrović ZS (2008) Polyurethanes from vegetable oils. *Polymer Reviews* **48(1)**: 109–155, https://doi.org/10.1080/15583720701834224.
22. PR Newswire (2015) Investment analysis of European adhesives and sealants market. *PR Newswire,* 13 April. See https://www.prnewswire.com/news-releases/investment-analysis-of-the-european-adhesives-and-sealants-2015-499563041.html (accessed 2023/07/11).
23. Zhang J, Severtson SJ and Lander MR (2015) *Pressure-Sensitive Adhesives Having High Bio-based Content and Macromonomers for Preparing Same*. US Patent US20150210907A1, Jul.
24. Pu G, Hauge DA, Gu C *et al.* (2013) Influence of acrylated lactide caprolactone macromonomers on the performance of high biomass content pressure-sensitive adhesives. *Macromolecular Reaction Engineering* **7(10)**: 515–726, https://doi.org/10.1002/mren.201300160.
25. Beharaj A, Ekladious I and Grinstaff MW (2019) Poly(alkyl glycidate carbonate)s as degradable pressure-sensitive adhesives. *Angewandte Chemie International Edition* **58(5)**: 1407–1411, https://doi.org/10.1002/anie.201811894.

26. Heinrich LA (2019) Future opportunities for biobased adhesives – advantages beyond renewability. *Green Chemistry* **21(8)**: 1866–1888, https://doi.org/10.1039/C8GC03746A.
27. Tarnavchyk I, Popadyuk A, Popadyuk N and Voronov A (2015) Synthesis and free radical copolymerization of a vinyl monomer from soybean oil. *ACS Sustainable Chemistry & Engineering* **3(7)**: 1618–1622, https://doi.org/10.1021/acssuschemeng.5b00312.
28. Demchuk Z, Shevchuk O, Tarnavchyk I *et al.* (2016) Free radical polymerization behavior of the vinyl monomers from plant oil triglycerides. *ACS Sustainable Chemistry & Engineering* **4(12)**: 6974–6980, https://doi.org/10.1021/acssuschemeng.6b01890.
29. Demchuk Z, Kohut A, Voronov S and Voronov A (2018) Versatile platform for controlling properties of plant oil-based latex polymer networks. *ACS Sustainable Chemistry & Engineering* **6(2)**: 2780–2786, https://doi.org/10.1021/acssuschemeng.7b04462.
30. Demchuk Z, Kirianchuk V, Kingsley K, Voronov S and Voronov A (2018) Plasticizing and hydrophobizing effect of plant oil based acrylic monomers in latex copolymers with styrene and methyl methacrylate. *International Journal of Theoretical and Applied Nanotechnology (IJTAN)* **6**: 29–37, https://doi.org/10.11159/ijtan.2018.005.
31. Kohut A, Voronov S, Demchuk Z *et al.* (2020) Non-conventional features of plant oil-based acrylic monomers in emulsion polymerization. *Molecules* **25(13)**: article 2990, https://doi.org/10.3390/molecules25132990.
32. Kirianchuk V, Domnich B, Demchuk Z *et al.* (2022) Plant oil-based acrylic latexes towards multisubstrate bonding adhesives applications. *Molecules* **27(16)**: article 5170, https://doi.org/10.3390/molecules27165170.
33. Neupane D, Lohaus RH, Solomon JKQ and Cushman JC (2022) Realizing the potential of *Camelina sativa* as a bioenergy crop for a changing global climate. *Plants* **11(6)**: article 772, https://doi.org/10.3390/plants11060772.
34. Chen C, Bekkerman A, Afshar RK and Neill K (2015) Intensification of dryland cropping systems for bio-feedstock production: evaluation of agronomic and economic benefits of *Camelina sativa*. *Industrial Crops and Products* **71**: 114–121, https://doi.org/10.1016/j.indcrop.2015.02.065.
35. Berti M, Gesch R, Eynck C, Anderson J and Cermak S (2016) Camelina uses, genetics, genomics, production and management. *Industrial Crops and Products* **94**: 690–710, https://doi.org/10.1016/j.indcrop.2016.09.034.
36. Arshad M, Mohanty AK, Van Acker R *et al.* (2022) Valorization of camelina oil to biobased materials and biofuels for new industrial uses: a review. *RSC Advances* **12(42)**: 27230–27245, https://doi.org/10.1039/D2RA03253H.
37. Mondor M and Hernandez-Alvarez AJ (2021) *Camelina sativa* composition, attributes, and applications: a review. *European Journal of Lipid Science and Technology* **124**: article 2100035, https://doi.org/10.1002/ejlt.202100035.
38. Zhang L, Cao Y, Wang L, Shao L and Bai Y (2016) Polyacrylate emulsion containing IBOMA for removable pressure sensitive adhesives. *Journal of Applied Polymer Science* **133(3)**: article 42886, https://doi.org/10.1002/app.42886.
39. Chen L, Bao Z, Fu Z and Li W (2015) Synthesis and characterization of novel cross-linking poly(butyl acrylate-*co*-isobornyl methacrylate) colloids prepared via semi-continuous seeded emulsion polymerization. *Colloid Journal* **77(3)**: 374–381, https://doi.org/10.1134/S1061933X15030059.
40. Knebel J and Saal D (2001) *Method for Synthesis and Process Inhibition of Isobornyl (Meth) Acrylate*. US Patent US6329543, Dec.
41. Meredith HJ and Wilker JJ (2015) The interplay of modulus, strength, and ductility in adhesive design using biomimetic polymer chemistry. *Advanced Functional Materials* **25(31)**: 5057–5065, https://doi.org/10.1002/adfm.201501880.
42. ASTM (2002) D 3330/D 3330M-02: Standard test method for peel adhesion of pressure-sensitive tape. ASTM International, West Conshohocken, PA, USA.
43. ASTM (2019) D 1002-10: Lap shear strength of adhesively bonded metal specimens. ASTM International, West Conshohocken, PA, USA.
44. Asua JM (2004) Emulsion polymerization: from fundamental mechanisms to process developments. *Journal of Polymer Science Part A: Polymer Chemistry* **42(5)**: 1025–1041, https://doi.org/10.1002/pola.11096.
45. Plessis C, Arzamendi G, Alberdi JM *et al.* (2002) Evidence of branching in poly(butyl acrylate) produced in pulsed-laser polymerization experiments. *Macromolecular Rapid Communications* **24(2)**: 173–177, https://doi.org/10.1002/marc.200390030.
46. Arzamendi G, Plessis C, Leiza JR and Asua JM (2003) Effect of intramolecular chain transfer to polymer on PLP/SEC experiments of alkyl acrylates. *Macromolecular Theory and Simulations* **12(5)**: 315–324, https://doi.org/10.1002/mats.200390030.